

EXPERIMENTAL STUDIES OF RC BEAM-SLAB STRUCTURES SUBJECT TO A PENULTIMATE-EXTERNAL COLUMN LOSS

Pham Xuan Dat, PE, Division of Structures and Mechanics, School of Civil and Environmental Engineering, Nanyang Technological University, Singapore
Tan Kang Hai, PhD, PE, Division of Structures and Mechanics, School of Civil and Environmental Engineering, Nanyang Technological University, Singapore

ABSTRACT

Progressive collapse resistance of reinforced concrete (RC) buildings can be evaluated by sudden column loss scenarios. The Penultimate-External (PE) column loss is among the most critical scenarios since it leaves the affected beam-slab structures with a horizontally unrestrained boundary condition. At large deformations, catenary tension forces in beams and slabs may pull inwards the corner column, accelerating progressive collapse. The main objective of the experimental programme described here is to study the static response of gravity-load-designed beam-slab substructures subject to a Penultimate column loss. Two 1/3 scale specimens have been designed, built, and tested by a static loading scheme. The boundary condition of the test specimens is rotationally restrained but laterally unrestrained. A twelve-point loading system is used to simulate the uniformly distributed load. It was observed that a peripheral compressive ring that is formed within the affected slabs can allow catenary action to develop without any inward lateral movement of the corner column until the central vertical deformation reached 6% of the double-span length. At large deformations, while the development of catenary action could enhance the overall load-carrying capacity, the gradual failure of beam-column connections together with fractures of beam bottom bars significantly reduced the capacity. Based on the test results, design and detailing recommendations to mitigate progressive collapse are discussed.

Keywords: Progressive Collapse, Penultimate-External Column Removal, Experimental Static Response of RC Beam-slab Substructures, Detailing and Design Recommendations.

1. INTRODUCTION

Progressive collapse resistance of a building structure can be evaluated by sudden column loss scenarios¹. The column to be removed may be an internal, external, or a corner column.

Following a sudden column removal, bending moments in beams and slabs bridging over the removed column are significantly increased by double-span effect and dynamic effect². The beam-column connections just above the removed column, which are initially designed for negative bending moment, now have to carry a huge positive bending moment. At the remote connections, negative bending moments, as a quadratic function of the double span length, may increase at least four times the initial values. If the affected beam-slab structures are not able to resist the increased bending moment, an alternative load path is needed to prevent progressive collapse.

Recent research has shown that catenary action carrying vertical loads by horizontal tension forces can be an alternative load path³. Under abnormal loading conditions such as sudden column loss when deformations become large, the compressive block in bending action in the double-span beams and slabs begins to unload significantly due to the excessive straining of tension longitudinal bars and concrete crushing of the compressive fibres, resulting in gradual failure of flexural mechanism. At this stage, catenary action starts developing. As long as the remaining reinforcement is continuous and there is sufficient lateral restraint to anchor the catenary tension forces, catenary capacity has been shown to be significantly higher than flexural capacity.

Sufficient lateral restraint, which is a vital condition for the development of catenary action, is not always available in an actual building structure. When an internal column is removed, this vital condition can be satisfied by a very strong horizontal diaphragm formed by adjacent slab panels surrounding the affected area associated with the removed column. However, when an ultimate column is removed, the amount of lateral restraint, which can only be provided by a peripheral compressive ring formed in the affected slabs bordered by two consecutive discontinuous edges, is less likely to meet the demand of the catenary action, resulting in a progressive collapse shown in Fig. 1. In such a situation, the catenary action may be a cause rather than a prevention of progressive collapse and penultimate column loss can be considered as among the most critical scenarios. It is worth noting that the number of Penultimate-External (PE) column loss scenarios basically depends on the structural layout of buildings. In a building with three bays and four spans shown in Fig. 1, the number of penultimate columns is up to 40% the total columns.

This paper presents an experimental programme that is conducted to investigate the static behaviour of RC building structures subjected to a PE column loss. Two one-third scaled beam-slab substructures were designed, built, and tested statically. Attention is paid to the development of catenary action together with the associated failure modes of the beam-slab structure. Based on the test results, several detailing and design recommendations are suggested. These recommendations are equally applicable to cast-in-place and precast building structures.

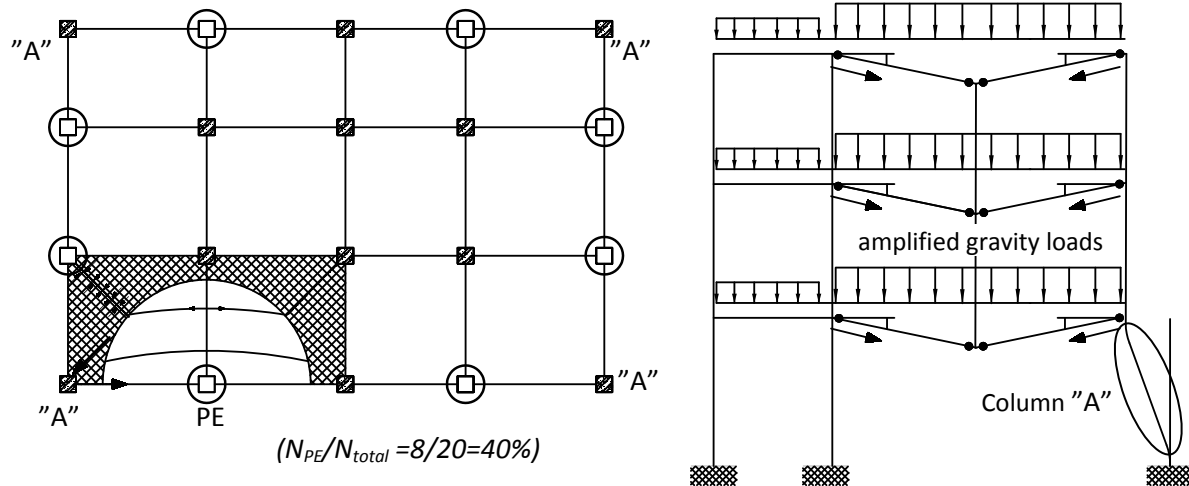


Fig. 1 Penultimate-External (PE) Column Loss and Typical Failure Mode

2. EXPERIMENTAL PROGRAMME

A test series was designed and tested statically at Nanyang Technological University, Singapore. The test specimens were a 1/3 scale model of a prototype building which was designed for gravity loading condition. The design live load was 3 kN/m² and the imposed dead load was 2 kN/m². In this paper, the test results of two specimens PE-01 SA and PE-02 SA are reported.

2.1 DESIGN OF SPECIMENS

Fig. 2 shows the detail of the two test specimens. Two slab aspect ratios ($a=1$) and ($a=1.4$) were used for PE-01 SA and PE-02 SA, respectively. Details of beams and slabs were kept the same for both specimens. In order to simulate two continuous edges, slabs and beams were extended 400 mm beyond the two consecutive perimeter beams. The extended slabs (the hatched areas) were 100 mm thick to avoid any torsional effects due to slab negative bending moment. Details of two specimens are summarized in Table 1.

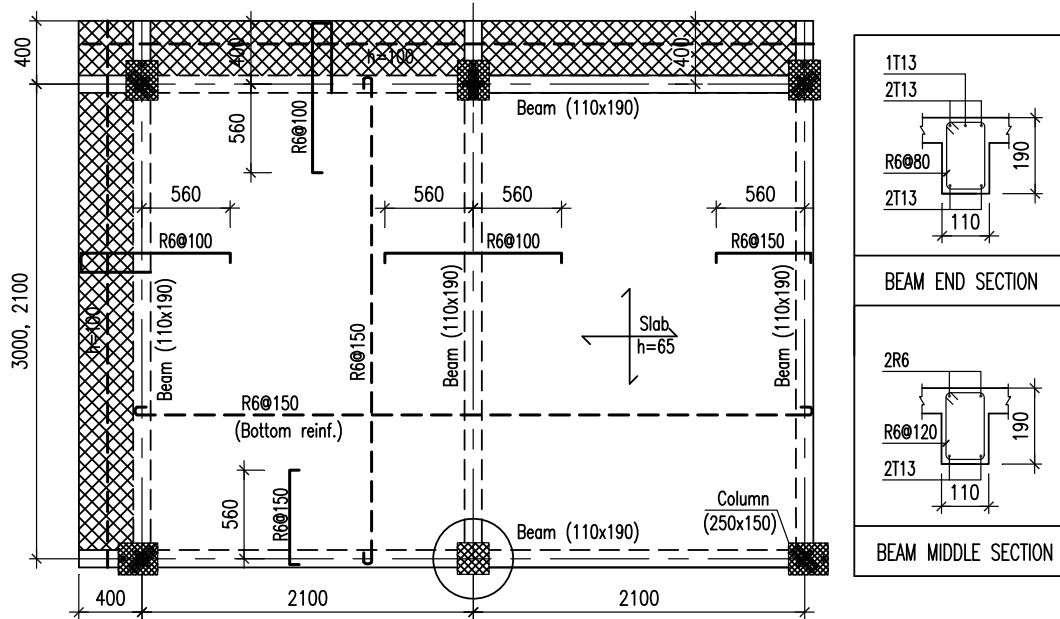


Fig. 2 Specimen Detail

Table 1: Details of test specimens

	Dimensions of slab panels (Aspect ratio)	Dimensions of beams	Overall dimensions	Bottom slab reinforcement	Top slab reinforcement
PE-01 SA	2100 x 2100 ($a = 1.0$)	110x190	2500x4600	$\Phi 6$ at 150 ($\rho_b = 0.38\%$)	$\Phi 6$ at 100/150 ($\rho_b = 0.57\%/0.76\%$)
PE-02SA	3000 x 4200 ($a = 1.4$)	110x190	3400x4600	$\Phi 6$ at 150 ($\rho_b = 0.38\%$)	$\Phi 6$ at 100/150 ($\rho_b = 0.57\%/0.76\%$)

Note: All dimensions are in mm; Strength of materials: $f'_c = 30$ MPa; $f_y = 460$ MPa

2.2 TEST SETUP

Test setups were designed based on two main assumptions. Firstly, the testing load is uniformly distributed. Following a sudden column removal, every floor above the removed column vibrates freely with its own gravity load, which is actually a uniform load. Secondly, a penultimate column removal may leave two consecutive edges of its associated beam-slab structures discontinuous. At large deformations, perimeter columns, which are able to continuously carry bending moments and axial forces, may not provide any lateral restraint to the slab or beam structures. Therefore, the boundary condition is considered as rotationally restrained but laterally unrestrained. The typical setup can be seen in Fig. 3. The test specimens were supported by five steel circular hollow section columns. Slab loads were applied by an actuator through a means of loading tree.

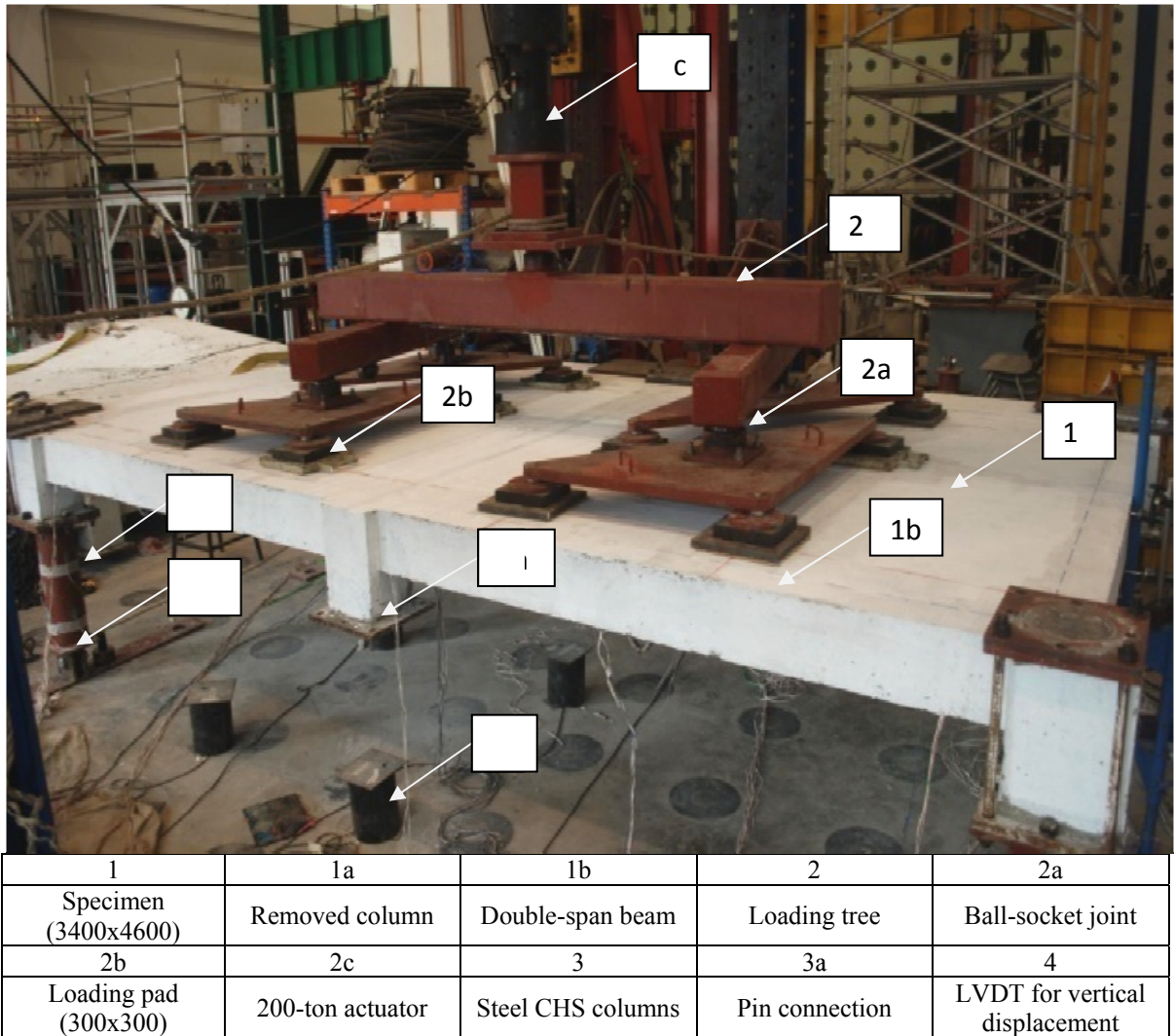


Fig. 3 A Typical Test Setup.

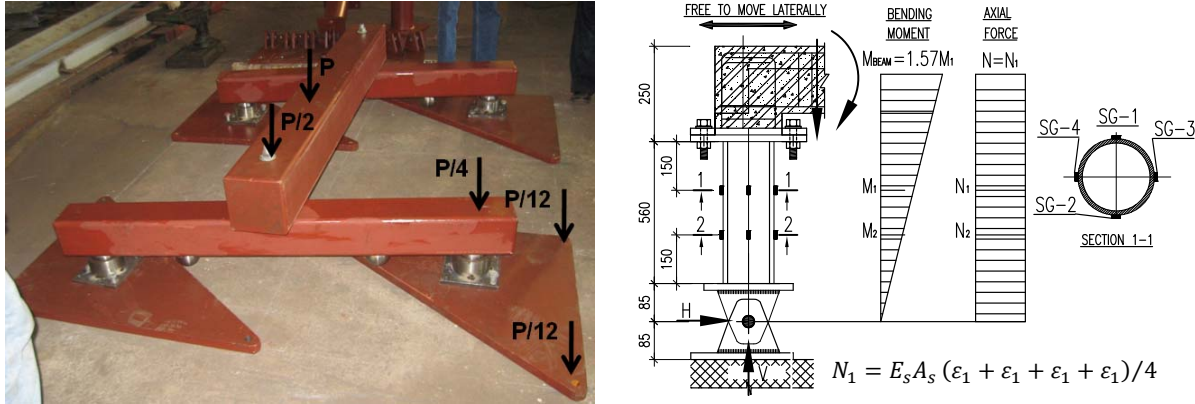
The Loading System

With a special emphasis on a uniformly distributed load applied onto the test structures, a loading scheme was designed based on existing laboratory constraints to reasonably simulate such loading condition. A 200-ton actuator which was held by a reaction steel frame placed across the specimen was used to load the specimens. The load from the actuator was distributed equally to twelve point loads by means of loading trees (Fig. 4a). Ball and socket joints between steel plates and steel rods were fabricated to keep the loading system as vertical as possible when specimens deformed excessively.

The Boundary Condition

As can be seen in Fig. 3, test specimens were supported by five steel hollow section columns. In order to fairly simulate the rotationally restrained but laterally unrestrained boundary

condition that represents the penultimate column loss scenarios one end of the steel columns was fully fixed to the specimen, while the other end was pin-connected to a 15 mm thick steel base plate that was securely fastened to the strong floor of the laboratory by two 40 mm diameter bolts. As shown in Fig. 4(b), the pin-ended columns allowed perimeter edges of specimens to move horizontally without any degree of lateral restraint.



a) Loading system

b) Supporting columns and reaction measurements

Fig. 4 Details of Loading System and Supporting Columns

Measurements

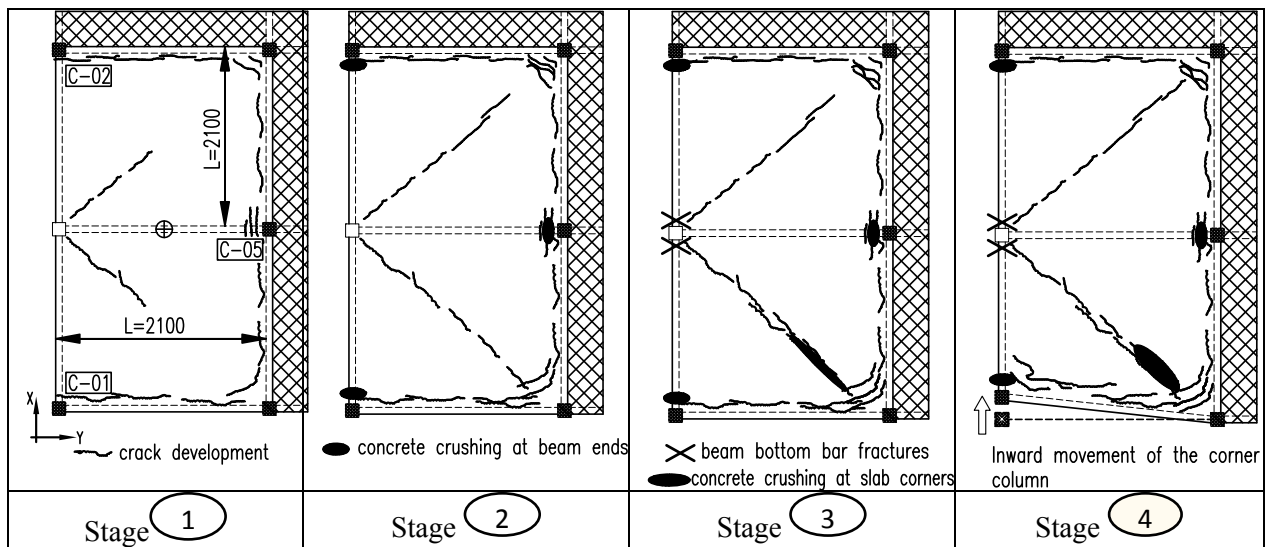
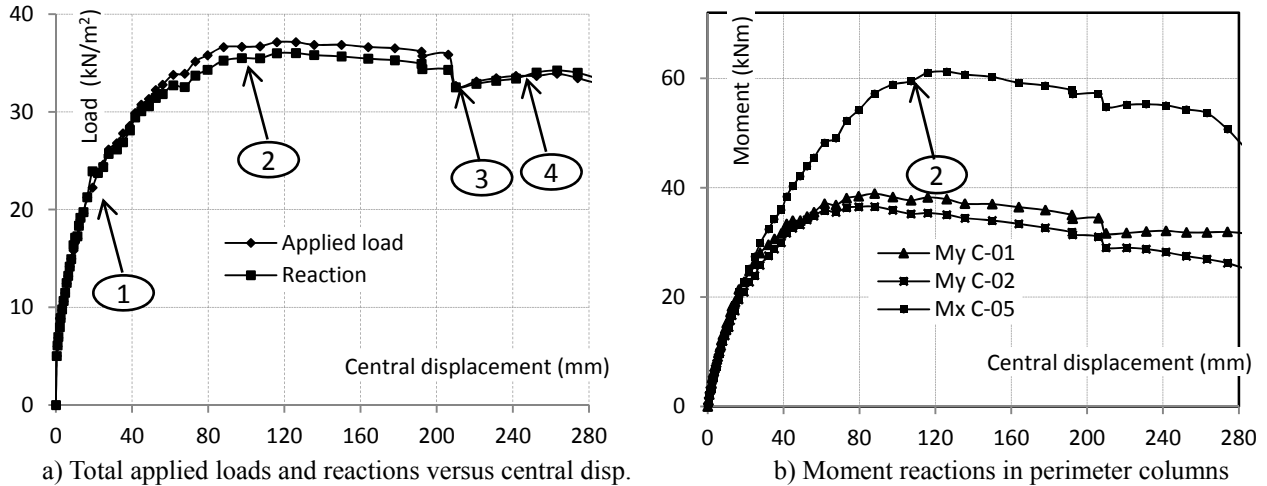
Concentrated loads from the actuator were measured by using an in-built load cell that was connected in series with the actuator. Vertical reaction forces and column bending moments in supporting columns were calculated through four strain gauges mounted on the opposing external surfaces of the columns as shown in Fig. 4(b). Both vertical and horizontal deformations of the specimens were measured using Line Transducers. Strain gauges mounted on beam and slab reinforcement at critical sections were used to identify the development of catenary action as well as the outer compressive ring.

Loading process

Specimens were statically tested to failure using a displacement-controlled test procedure. The incremental displacement of 1 mm is used until the specimens completely failed.

2.3 TEST RESULTS AND OBSERVATIONS

Specimen PE-01 SA ($L_x=2100$, $L_y=2 \times 2100$, $\rho_{top\ slab} = 0.22\%$, $\rho_{bottom\ slab} = 0.44\%$)



c) Four stages depicting the main experimental observations

Fig. 5 Measurements and Experimental Observations of Specimen PE-03

Fig. 5 shows the experimental behaviour of Specimen PE-01 SA, including (a) the relationship between the applied load and the vertical displacement measured at the middle of the double-span beam, or at the removed column position, (b) bending moment obtained from three main supporting columns C-01, 02, 05 using the moment profile, and (c) four stages depicting the main experimental observations. After reaching a peak value of $37kN/m^2$ at a central displacement of 90 mm, the test load remained stable until the displacement attained 200 mm, which is 5% of the double-span length. Fractures of bottom bars of the double-span beam caused a sudden reduction in a uniform load of $4kN/m^2$ at a displacement of 220 mm (Stage 3). At the bottom faces of the ends of the double span beam, concrete was observed to start crushing at a displacement of 100 mm (Stage 2). Since then the crushing was continuous with an increase of displacement, leading to gradual reduction in moment reactions from C-01, 02, 05 (Fig. 5b). It was noted that the moment reaction obtained from column C-02 (with slab extension) was identical to that from the corner column C-01

(without slab extension), indicating no torsional effect on the perimeter beam caused by slab negative bending moment.

The corner column C-01 started moving inwards under tension catenary forces at a central displacement of about 260 mm, 6.3% of the double-span length. The final failure of this specimen can be seen in Fig. 6.

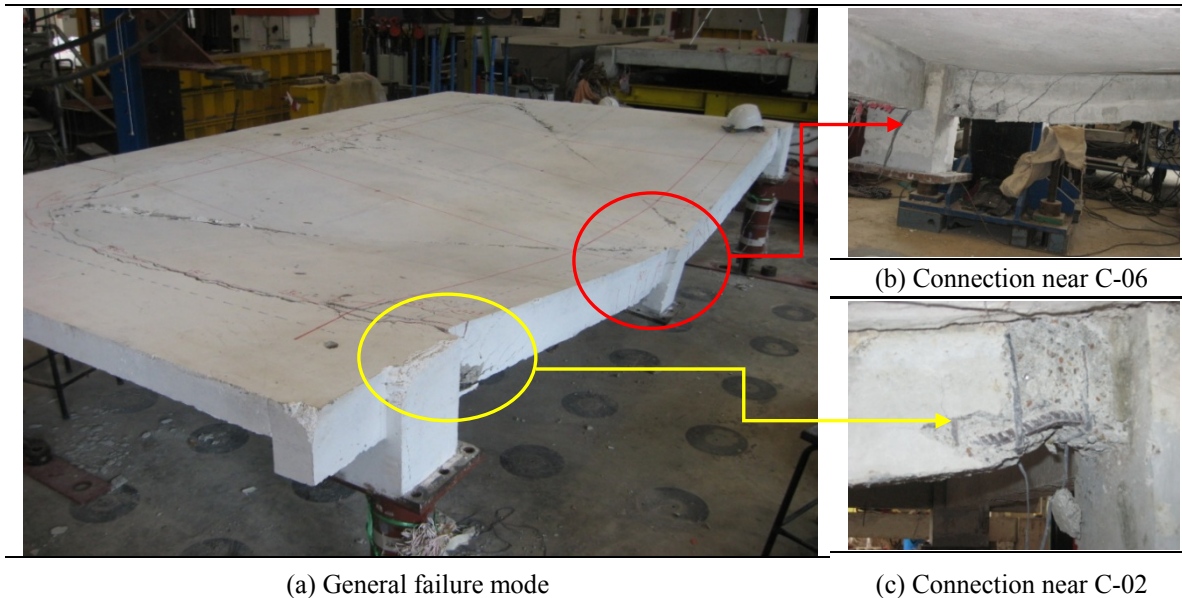
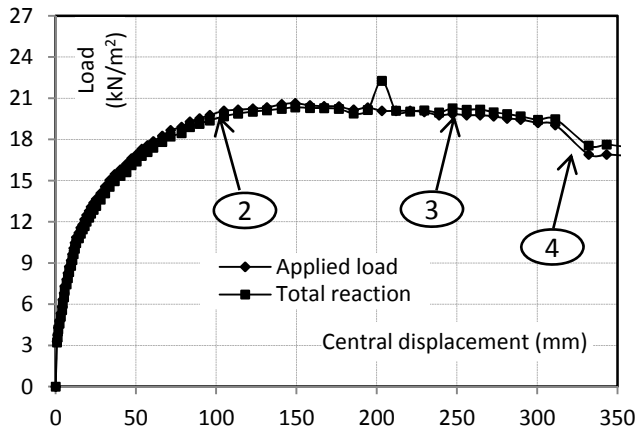


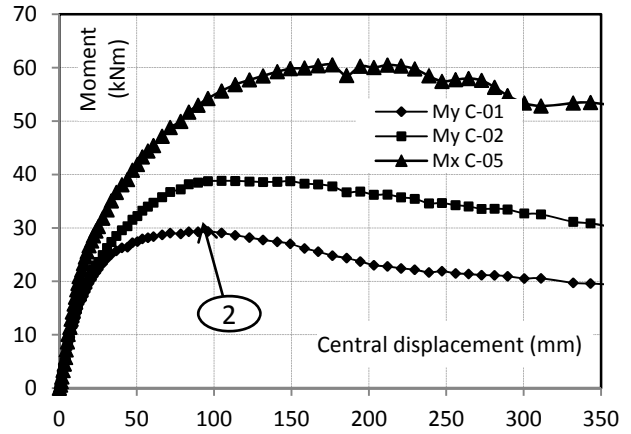
Fig. 6 Failure Mode of Specimen PE-02 SA

Specimen PE-02 SA ($L_x=2100$, $L_y=2 \times 2100$, $\rho_{top\ slab} = 0.22\%$, $\rho_{bottom\ slab} = 0.44\%$)

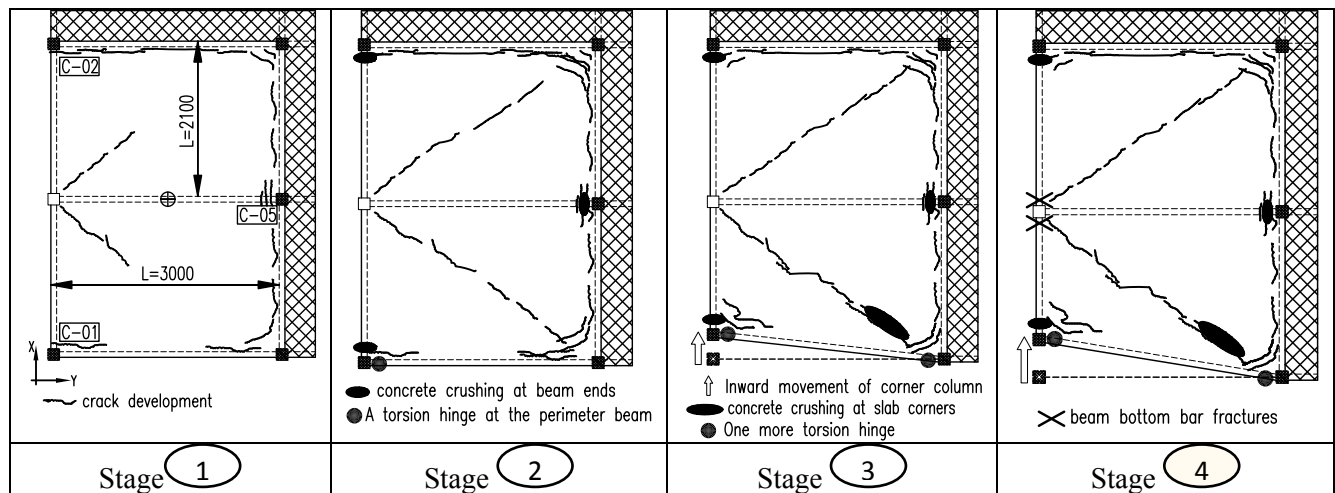
Experimental phenomena observed in PE-02 SA is shown in Fig. 7. The test behaviour is basically similar to that observed in PE-01SA, namely, a stable trend of the load-carrying capacity versus the central displacement, partial failures such as fracture of beam bottom bars, crushing and spalling of concrete and the inward movement of the corner columns after the failure of the compressive ring. There are two differences which have been observed: (i) the presence of torsional failure of the perimeter edge beam due to slab negative bending moment at the ends of the double-span beam, and (ii) fracture of beam bottom bars of the double span beam occurred after the inward movement of the corner column C-01 (Stages 3 and 4). The corner column C-01 started moving inwards under tension catenary forces at a central displacement of about 250 mm, 6.1% of the double-span length. The torsional failure caused the moment reaction obtained from corner column C-01 (without slab extension) to occur at a significantly smaller applied load than that obtained from column C-02 (with slab extension) described in Fig. 7b. The final failure of the specimen as well as the perimeter beam can be seen in Fig. 8.



a) Total applied loads and reactions versus central disp.



b) Moment reactions in perimeter columns



(c) four stages depicting the main experimental observations

Fig. 7: Measurements and Experimental Observations of Specimen PE-02 SA



Fig. 8 Failure Mode of Specimen PE-02 SA

Fig. 9 shows strain gauge readings versus the central vertical displacement at two critical sections of the double-span beam of PE-02 SA. At the section near the face of column C-02, while the tensile strain in the top reinforcement T-2 was stable at about 7000μ , the compressive strain in the bottom reinforcement B-2 decreased significantly after reaching the first peak of 1500μ at a displacement of 100 mm , then the bar strain changed and became tensile at a displacement of 250 mm . This change was due to concrete crushing at the bottom face of the beam section under negative bending moment. Strain readings at the section near the face of the removed column C-06 showed the development of catenary action in the beam. As can be seen in Fig. 9(b) while the tensile strain B-6 became stable at about 4200μ before it failed at a displacement of 120 mm , the compressive strain T-6 in the top reinforcement after getting a peak value of 120μ at a displacement of 15 mm changed to tensile strain at a displacement of about 25 mm . After that the tensile strain increased gradually up to 1000μ at a displacement of 250 mm . It is obvious that not only the top reinforcement of the double-span beam but the top and bottom reinforcement of slabs in this region could also contribute to catenary action. It is to be noted that the bottom bars attached with tensile strain B-6 fractured at a displacement of 300 mm (Stage 4 in Fig. 7a)

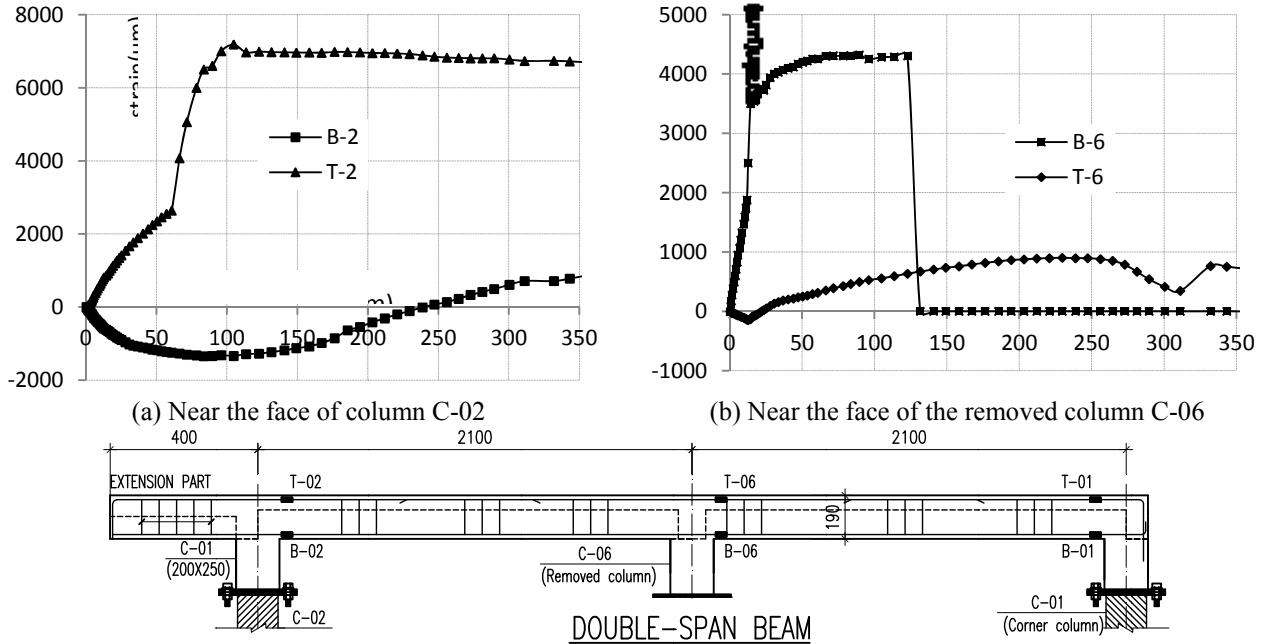


Fig. 9 Strain Gauge Readings of The Double-span Beam

2.4 LOAD-CARRYING CAPACITIES OF THE TEST SPECIMENS

At small displacement, the beam-slab specimens carried applied gravity loads by negative bending moment along the perimeter edges combined with positive bending moment in the central area. When the vertical displacement becomes large, the positive bending moment was gradually replaced by catenary action carrying the applied loads by tension mode, as shown in Fig. 9(b). While catenary capacity increased proportionally, negative bending capacity tended to decrease due to partial failures such as the concrete crushing at the bottom face of the beam-perimeter column connections (Fig. 9a) and the torsional failure of perimeter beams under slab negative bending moment (Fig. 8). As can be seen in Figs. 5(a) and 6(a), the load-carrying capacities of the specimens, instead of being either proportional or disproportional to the vertical displacement, became stable until the corner column moved inwards at a vertical displacement of more than 6% of double span length.

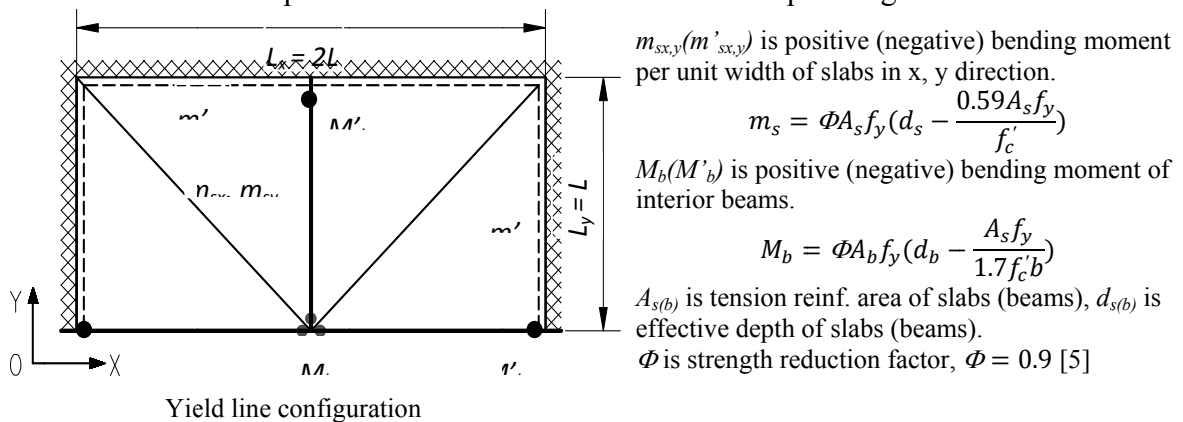


Fig. 10 Summary of Yield-line Calculation

Yield-line analysis is used to calculate the ultimate flexural capacity (w_{ult}) of the beam-slab substructures based on the yield-line patterns shown in Figs. 6 and 8. The yield-line calculation for PE-01 SA is summarized in Fig. 10, the virtual work equation may be written as:

$$\sum W_{ult}\Delta = (2m_{sx}L + 2m_{sy}L + 2m'_{sx}L + 2m'_{sy}L)\theta + (3M_b + 3M'_b)\theta \quad (\text{Eq. 1})$$

The external virtual work due to uniform load (w_{ult}) can be expressed:

$$\sum W_{ult}\Delta = 4w_{ult} \frac{\delta}{3} L L \frac{1}{2} = 2w_{ult}\delta L^2/3 (\text{Eq. 2})$$

Using compatibility condition of deformation: $\theta = \frac{\delta}{L}$, then we have

$$w_{ult} = \frac{3}{L^2} (m_{sx} + m_{sy} + m'_{sx} + m'_{sy}) + \frac{4.5}{L^3} (M_b + M'_b) \quad (\text{Eq. 3})$$

The same procedure can be applied to PE-02 SA with $L_y = 1.4L$

Table 2: Load-carrying capacities of the test specimens predicted by Eq.3

	L_x/L_y (mm)	m_{sx}/m_{sy} (kNm/m)	m'_{sx}/m'_{sy} (kNm/m)	M_b/M'_b (kNm)	w_{ult} (kN/m ²)
PE-01 SA	4200/2100	3.4/3.4	5.7&4.1/4.1	9.5/23.6	26.3
PE-02 SA	4200/3000	3.4/3.4	5.7&4.1/4.1	9.5/23.6	17.9

Note: Concrete cover for slabs & beams are 12&15 mm

Table 3: Comparisons between the test loads and the predicted load-carrying capacities

	w_{ult} (kN/m ²)	w_{peak} (kN/m ²)	$w_{failure}$ (kN/m ²)	w_{peak}/w_{ult}	$w_{failure}/w_{ult}$
	(1)	(2)	(3)	(4)=(2)/(1)	(5)=(3)/(1)
PE-01 SA	26.3	37.3 (at 120 mm)	33.7 (at 240 mm)	1.42	1.29
PE-02 SA	17.9	21.1 (at 100 mm)	20.6 (at 250 mm)	1.18	1.15

Table 2 shows the load-carrying capacities predicted by Eq.3 and Table 2 shows the comparisons between the predicted capacities and test loads. The failure loads are determined when the corner columns started moving inwards. As can be seen in Table 3, the failure loads are significantly higher than the predicted values despite fractures of bottom bars as well as compressive failure of interior beam-column happening at large deformations. Due to the torsional failure of the perimeter beam under slab negative bending moment (Fig. 8) the discrepancy between the test load and the predicted value in PE-02 SA test is less than that obtained from PE-01 SA test.

It has been found that for beam-slab structures the test loads were often greater compared with the ultimate flexural capacity predicted by traditional yield-line approach⁶. This is due to the T-beam effect on the negative bending moment defined as some of slab reinforcing bars in the overhanging flanges acted as tension steel together with the longitudinal reinforcing bars of interior beams, resulting in a significantly greater negative bending capacity.

3. DESIGN AND DETAILING RECOMMENDATIONS

3.1 DESIGN RECOMMENDATION

In order to assess progressive collapse resistance of RC building structures, the most recent document UFC 4-023-03 published by United States Department of Defense (DoD) has introduced a nonlinear static analysis procedure. In this procedure the nonlinear response of the affected structures associated with a removed column is evaluated by numerical modelling using an advanced software and the dynamic effect on the gravity loads on the floor areas directly above the removed column can be quantified as¹;

$$\Omega_{Nonlinear} = 1.04 + 0.45/(\theta_{pra}/\theta_y + 0.48) \quad (Eq.4)$$

where $\Omega_{Nonlinear}$ is the dynamic increase factor for non-linear analysis. θ_y , θ_{pra} are the yield rotation angle and plastic rotation angle of the structural element (beam, slab) connected to the affected floor area. The smallest ratio of θ_{pra}/θ_y is chosen for any primary element to obtain the largest value of dynamic increase factor for the overall structural analysis.

While the evaluation of dynamic increase factor Ω is quite straightforward, that of the nonlinear static response of the affected structures is complicated and very time-consuming. Firstly, it requires the designer to be familiar to a relatively complicated multi-step analysis in which every step must be conducted with an advanced software. Secondly, in creating a structural model of the entire building structure, load-deformation behaviour of all structural elements such as beams, slabs and connections should be explicitly modeled, including the strength degradation as well as residual strength. It seems that this procedure is only suitable for DoD facilities when progressive collapse mitigation is among the top priorities. For ordinary facilities such as residential or office buildings, a simple yet conservative approach is needed.

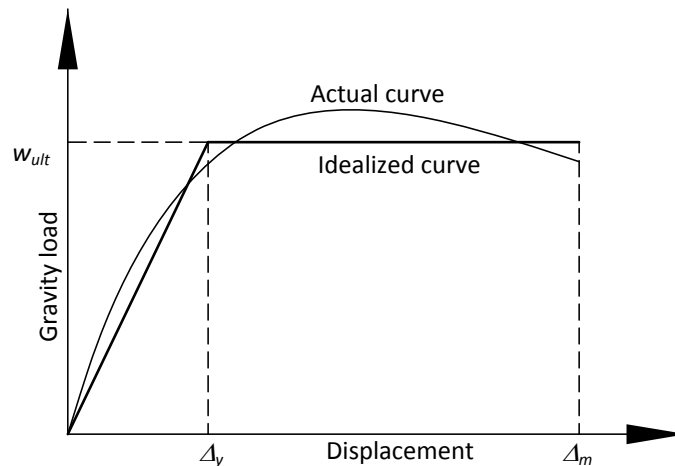


Fig. 10 Elastic-Plastic Response of Beam-Slab Structure

Based on the current test results, it has been shown that the ultimate load-carrying capacity of a affected beam-slab structure associated with a column removal can be conservatively predicted by yield-line approach. Therefore, the nonlinear response of the beam-slab structure can be idealized by elastic-plastic relationship, as shown in Fig. 11.

It is common that in precast building systems beams and slabs of every floor are typically designed so that every floor is considered approximately identical in terms of gravity load, strength and stiffness. Under a sudden column loss scenario, the associated floors possessing the same gravity load, strength and stiffness will go into identical vertical vibration². As a result, the progressive collapse resistance of the building structures can be assessed by considering only a typical floor, given as:

$$w_{al} = \frac{w_{ult}}{\Omega} \quad (Eq.5)$$

where: w_{al} is the allowable gravity load applied on a typical floor. w_{ult} is the static ultimate flexural load-carrying capacity of the beams and slabs bridging over the removed column, which is predicted by yield-line approach. Ω is the dynamic increase factor obtained from Eq. 4.

3.2 DETAILING RECOMMENDATION

For the development of catenary action to be considered as a alternative load path for mitigating progressive collapse under column loss scenarios, the continuity of longitudinal bars of beams and slabs through beam-column connections is a vital condition. This condition, which is less likely to be satisfied in precast beam-slab systems, has to be provided by other independent means. Topping slab construction and beam shoes for precast beams are among the feasible solutions. From the strain gauge profiles shown in Fig. 9(b), the lower the additional longitudinal bars are from the top surface of the floor, the better the development of catenary action. Therefore, the use of additional bars with sufficient tension anchorage placed in the beam shoes as well as in the bottom of the topping layer are recommended.

Under the penultimate column loss scenario, the inward movement of the corner column which may possibly cause collapse of affected structures is due to concrete crushing at slab corners, as can be seen in Figs. 5 and 7. Therefore, the use of additional reinforcement in the top of the topping layer at the beam-column connection is also recommended to strengthen the slab corners.

4. SUMMARY

This paper presented an experimental investigation of static response of RC beam-slab structures subjected to a Penultimate-External column loss. Test setup and instrumentation have been discussed together with several experimental observations, including: the development of of catenary action, the failure of flexural action, and the final failure mode of test specimens. Based on the test results, a simplified approach is proposed to quickly estimate the progressive collapse resistance, in which the static ultimate flexural load-carrying capacity of the beams and slabs bridging over the removed column is predicted by yield-line approach. Detailing recommendations to mitigate progressive collapse of precast structures are also discussed.

REFERENCES

1. Unified facilities criteria (UFC) by United states Department of Defense (DoD)
2. Tan Kang Hai, Pham Xuan Dat, "Membrane actions of RC slabs in mitigating progressive collapse of building structures", *The third international conference on design and analysis of protective structures*, 10-12 May 2010, pp. 105-115.
3. Sasani, M., and Kropelnicki, J. "Progressive collapse analysis of an RC structure" *The Structural Design of Tall and Special Buildings*, 2007
4. Colin Gurley "Progressive Collapse and Earthquake Resistance", *Practice Periodical on Structural Design and Construction*, Vol. 13, No. 1, February 1, 2008
5. Park, R., and Gamble, W. L. (2000), *Reinforced Concrete Slabs*, John Wiley & Sons, Inc.
6. Pham Xuan Dat, Tan Kang Hai "Experimental studies of RC beam-slab structures subjected to a Penultimate - Internal column loss", to be published.